

# Synthesis of Cage Compounds Containing Boron, Tin, and Phosphorus Atoms

Tuqiang Chen,<sup>†</sup> Eileen N. Duesler,<sup>†</sup> Robert T. Paine,<sup>\*,†</sup> and H. Nöth<sup>\*,†</sup>

Department of Chemistry, University of New Mexico, Albuquerque, New Mexico 87131, and Institut für Anorganische Chemie, Universität München, 80333 München, Germany

Received October 24, 1996<sup>⊗</sup>

The 1:1 reactions of [ $(i\text{-Pr}_2\text{N})\text{BP}(\text{H})\text{B}(\text{N}^i\text{Pr}_2)\text{PLi}\cdot\text{DME}$ ] (**1**) and [(tmp)BP(H)B(tmp)PLi·DME] (**2**; tmp = 2,2,6,6-tetramethylpiperidino) with organylhalostannanes have been examined, and stannyl-substituted diphosphadiboretanes,  $(\text{R}_2\text{N})\text{BP}(\text{H})\text{B}(\text{NR}_2)\text{PSn}(\text{Cl})\text{R}'_2$  ( $\text{R}_2\text{N} = i\text{-Pr}_2\text{N}$ , tmp;  $\text{R}' = \text{Me}$ ,  $t\text{-Bu}$ ) have been isolated and characterized. Dehydrohalogenation of these compounds with  $t\text{-BuLi}$  produced bicyclic cage compounds  $\text{P}_2(\text{R}_2\text{NB})_2\text{SnR}'_2$  ( $\text{R}_2\text{N} = i\text{-Pr}_2\text{N}$  (**9**), tmp (**8**);  $\text{R}' = t\text{-Bu}$ ) or an oligomer  $[-\text{P}(\text{R}_2\text{NB})_2\text{PSn}(\text{R}'_2)-]$  ( $\text{R}_2\text{N} = \text{tmp}$ ;  $\text{R}' = \text{Me}$ ). The 2:1 reactions of  $\text{R}'_2\text{SnCl}_2$  with **1** and **2** have been studied, and with a small  $\text{R}'$  group (Me) a disubstitution product,  $[\text{HP}(\text{tmpB})_2\text{P}]_2\text{SnMe}_2$  (**11**), is obtained. With a larger  $\text{R}'$  group ( $t\text{-Bu}$ ), cage products  $\text{P}_2(\text{tmpB})_2\text{Sn}^i\text{Bu}_2$  and  $\text{P}_2(i\text{-Pr}_2\text{NB})_2\text{Sn}^i\text{Bu}_2$  are isolated. The molecular structures of **8** and **9** have been determined by single crystal X-ray diffraction techniques, and these structures and their spectroscopic features are discussed in relation to other boron–phosphorus cage compounds.

## 1. Introduction

A systematic approach for the preparation of bicyclic cage compounds containing boron and phosphorus atoms has been developed that utilizes small ring compounds as construction components and addition and elimination reactions on these rings to develop the cage structure, as summarized in Scheme 1.<sup>1</sup> Recently, this chemistry has been extended to cage species containing B, P, and Si atoms<sup>2</sup> and B, P, and Ge atoms.<sup>3</sup>

In this report, the parallel chemistry involving the construction of cages containing B, P, and Sn atoms is described.<sup>4</sup>

## Experimental Section

**General Information.** Standard inert-atmosphere techniques were used for the manipulation of all reagents and reaction products. Infrared spectra were recorded on a Matteson 2020 FT-IR from KBr pellets. Mass spectra were obtained from a Finnegan GC/MS using the solids inlet probe or on a Kratos MS-50 spectrometer with FAB analysis. NMR spectra were recorded on Bruker WP-250 and JEOL GSX-400 spectrometers, and the data are summarized in Table 1. The spectra were referenced with  $\text{Me}_4\text{Si}$  ( $^1\text{H}$ ,  $^{13}\text{C}$ ),  $\text{F}_3\text{B}\cdot\text{OEt}_2$  ( $^{11}\text{B}$ ), 85%  $\text{H}_3\text{PO}_4$  ( $^{31}\text{P}$ ), and  $\text{Et}_4\text{Sn}$  ( $^{119}\text{Sn}$ ) with  $+d$  being downfield from the reference. The samples were contained in sealed 5 mm tubes and dissolved in a deuterated lock solvent. Elemental analyses were determined at the University of New Mexico microanalysis facility.

**Materials.** Reagents  $i\text{-Pr}_2\text{NBCl}_2$ ,<sup>5</sup> (tmp)BCl<sub>2</sub>,<sup>6</sup> LiPH<sub>2</sub>·DME,<sup>7</sup>  $i\text{-Pr}_2\text{-NBP}(\text{H})(i\text{-Pr}_2\text{NB})\text{PLi}\cdot\text{DME}$ ,<sup>2,8</sup> (**3**), and (tmp)BP(H)(tmpB)PLi·DME<sup>8</sup> (**4**)

were prepared as described in the literature.  $\text{Me}_2\text{SnCl}_2$  and  $t\text{-Bu}_2\text{SnCl}_2$  were purchased from Strem Chemical Co. Solvents were rigorously dried and degassed by standard methods. Solvent transfers were accomplished by vacuum distillation, and all reactions and product workups were performed under dry nitrogen.

**Synthesis and Characterization of Compounds. 2,4-Bis(dialkylamino)-1-(diorganochlorostannyl)-1,3-diphospha-2,4-diboretanes 5–7.** Each of these compounds was prepared in a similar fashion. A solution of  $\text{Me}_2\text{SnCl}_2$  (0.24 g, 1.1 mmol) in toluene (30 mL) was cooled to  $-78^\circ\text{C}$ , and a solid sample of **4** (0.50 g, 1.1 mmol) was added. The mixture was stirred at  $-78^\circ\text{C}$  (2 h) and then at  $23^\circ\text{C}$  (16 h). The resulting cloudy orange mixture was filtered and solvent removed from the filtrate by vacuum evaporation. The remaining orange solid **5** was recrystallized from pentane (5 mL) at  $-10^\circ\text{C}$ : yield, 0.37 g (62%); mp  $142\text{--}144^\circ\text{C}$  (dec). Compounds **6** and **7** were prepared in an identical manner except that the reactions were performed in hexane. Compound **6** was obtained as an orange solid: yield, 0.76 g (79%) from 1.5 mmol each of **4** and  $t\text{-Bu}_2\text{SnCl}_2$ ; mp  $179\text{--}181^\circ\text{C}$ . Compound **7** was obtained as an orange viscous oil that solidified upon standing: yield 0.43 g (100%) from 0.79 mmol each of **3** and  $t\text{-Bu}_2\text{SnCl}_2$ ; mp  $64\text{--}68^\circ\text{C}$ .

**Characterization Data.** Compound **5**. Mass spectrum (30 eV) [ $m/e$  (%): 514 ( $\text{M}^+ - \text{Cl}$ , 1%), 499 ( $\text{M} - \text{Cl} - \text{CH}_3^+$ , 1%), 365 ( $\text{M} - \text{SnClMe}_2^+$ , 100%). Infrared spectrum (KBr,  $\text{cm}^{-1}$ ): 2961 (s), 2938 (s), 2868 (m), 2247 (m), 1464 (m), 1368 (s), 1331 (s), 1300 (m), 1242 (w), 1163 (m), 1128 (m), 1040 (w), 988 (m), 856 (w), 762 (m), 700 (w), 575 (w), 540 (w), 519 (w), 498 (w). Anal. Calcd for  $\text{C}_{20}\text{H}_{43}\text{N}_2\text{B}_2\text{P}_2\text{SnCl}$  (549.26): C, 43.73; H, 7.89; N, 5.10. Found: C, 44.23; H, 7.79; N, 4.95. Compound **6**. Mass spectrum (30 eV) [ $m/e$  (%): 631–636 ( $\text{M}^+$ , 1%), 594–601 ( $\text{M} - \text{Cl}^+$ , 5%) 572–587 (10%). Infrared spectrum (KBr,  $\text{cm}^{-1}$ ): 2961 (s), 2930 (s), 2851 (s), 2238 (m), 1464 (m), 1370 (s), 1327 (s), 1304 (m), 1244 (w), 1161 (s), 1128 (m), 1043 (w), 990 (m), 860 (w), 804 (w), 704 (w), 571 (w), 547 (w). Anal. Calcd for  $\text{C}_{26}\text{H}_{55}\text{N}_2\text{B}_2\text{P}_2\text{Cl}_2\text{Sn}$  (633.42): C, 49.30; H, 8.75; N, 4.42. Found: C, 49.60; H, 8.92; N, 4.25. Compound **7**. Mass spectrum (30 eV) [ $m/e$  (%): 493–500 ( $\text{M} - t\text{-Bu}$ , 15%), 401–405 ( $\text{M} - 2t\text{-Bu} - \text{Cl}^+$ , 34%). Infrared spectrum (KBr,  $\text{cm}^{-1}$ ): 2967 (s), 2928 (s), 2847 (s), 2715 (s), 2278 (m), 1466 (s), 1443 (s), 1366 (s), 1310 (s), 1184 (s), 1155 (s), 1005 (m), 870 (w), 801 (w), 577 (w), 544 (w), 500 (w).

**2,4-Bis(dialkylamino)-5,5-di-tert-butyl-1,3-diphospha-2,4-diboro-5-stannabicyclo[1.1.1]pentanes 8 and 9.** A solution containing **6** (1.40

<sup>†</sup> University of New Mexico.

<sup>‡</sup> Universität München.

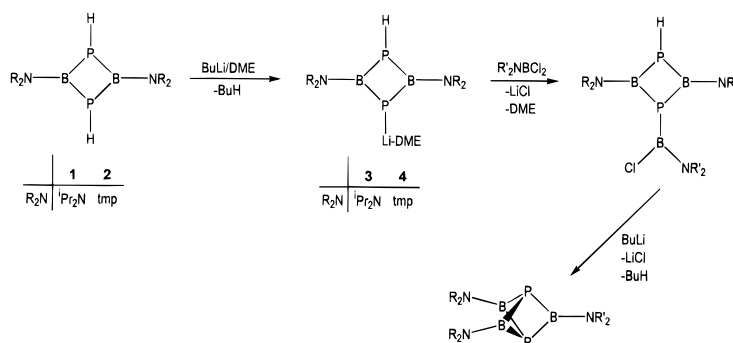
<sup>⊗</sup> Abstract published in *Advance ACS Abstracts*, February 15, 1997.

- (1) Dou, D.; Wood, G. L.; Duesler, E. N.; Paine, R. T.; Nöth, H. *Inorg. Chem.* **1992**, *31*, 3756.
- (2) Dou, D.; Kaufmann, B.; Duesler, E. N.; Chen, T.; Paine, R. T.; Nöth, H. *Inorg. Chem.* **1993**, *32*, 3056.
- (3) Chen, T.; Duesler, E. N.; Paine, R. T.; Nöth, H. *Inorg. Chem.*, submitted for publication.
- (4) Abbreviations used in the text include tmp = 2,2,6,6-tetramethylpiperidino, Me = methyl, tms = trimethylsilyl, THF = tetrahydrofuran,  $i\text{-Pr}$  = isopropyl, DME = ethylene glycol dimethyl ether, and  $t\text{-Bu}$  = *tert*-butyl.
- (5) Gerrard, W.; Hudson, H. R.; Mooney, E. R. *J. Chem. Soc.* **1960**, 5168.
- (6) Nöth, H.; Weber, S. Z. *Naturforsch., B* **1983**, *37*, 1460.
- (7) Schäfer, H.; Fritz, G.; Hölderich, W. Z. *Anorg. Allg. Chem.* **1977**, *428*, 222.
- (8) Dou, D.; Westerhausen, M.; Wood, G. L.; Linti, G.; Duesler, E. N.; Nöth, H.; Paine, R. T. *Chem. Ber.* **1993**, *126*, 379.

**Table 1.** NMR Spectroscopic Data (23 °C, C<sub>6</sub>D<sub>6</sub>)

compd <sup>a</sup>	<sup>11</sup> B{ <sup>1</sup> H}	<sup>31</sup> P{ <sup>1</sup> H}	<sup>119</sup> Sn{ <sup>1</sup> H}	<sup>1</sup> H	<sup>13</sup> C{ <sup>1</sup> H}
<b>1</b>	47.1	-162.8		3.9 (PH) 1.1 (CH <sub>3</sub> )	51.6 (CH) 23.2 (CH <sub>3</sub> ) 3.5
<b>2</b>	50.8	-127.2		4.7 (PH) 1.52 (tmp)	58.2, 40.9 30.2, 33.4 16.4 (tmp)
<b>3</b>	50.0	-174.9 -91.2		4.41 (PH) 4.12 (CH), 3.78 (CH') 3.39, 3.2 (DME) 1.45 (CH <sub>3</sub> ), 1.38 (CH <sub>3</sub> ') <sup>†</sup>	70.7, 59.4 (DME) 50.6 (CH), 49.3 (CH') 24.8 (CH <sub>3</sub> ), 23.5 (CH <sub>3</sub> ') <sup>†</sup>
<b>4</b>	53.6	-138.3 -15.5		3.38, 3.13 (DME) 1.93, 1.65 (tmp)	57.0, 44.5, 33.3, 17.5 (tmp)
<b>5</b>	49.9	-129.2 -113.1	75.1	5.75 (PH) 1.63, 1.36, 1.32 (tmp) 0.93 (SnMe <sub>2</sub> )	58.4, 41.6 32.9, 16.2 (tmp) 1.2 (SnMe <sub>2</sub> )
<b>6</b>	51.4	-136.3 -105.2	74.9	5.79 (PH) 1.57 (CMe <sub>3</sub> )	58.4, 42.8 36.5, 34.5 30.5, 16.4 (tmp) 41.8 (CMe <sub>3</sub> ) 31.6 (CMe <sub>3</sub> )
<b>7</b>	49.8 <sup>b</sup>	-184.3 -147.0	99.5	4.96 (PH) 4.26, 3.23 (CH) 1.43 (Sn <sup>t</sup> Bu) 1.24, 1.08 (CHMe <sub>2</sub> )	55.3, 47.5 (CH) 41.1 (CMe <sub>3</sub> ) 30.7 (CMe <sub>3</sub> ) 24.6, 22.2 (CHMe <sub>2</sub> )
<b>8</b>	49.7	50.1	-277.0	1.99, 1.73 1.6 (tmp) 1.50 (CMe <sub>3</sub> )	58.2, 40.9 34.7, 32.8 15.9 (tmp) 37.9 (CMe <sub>3</sub> ) 33.8 (CMe <sub>3</sub> )
<b>9</b>	49.1	-12.7	-197.1	4.02 (CH) 1.43 (CMe <sub>3</sub> ) 1.32, 1.28 (CHMe <sub>2</sub> )	
<b>10</b>		-100 to -150			
<b>11</b>	52.6	-127.9 -107.3	26.2	5.74 (PH) 1.71-1.44 (tmp) 1.15 (Me <sub>2</sub> Sn)	58.1, 42.4 31.9, 23.0 16.6, 14.3 (tmp) -2.3 (Me <sub>2</sub> Sn)

<sup>a</sup> Coupling constants (Hz): **5**, <sup>1</sup>J<sub>PSn</sub> = 920 (<sup>119</sup>Sn), 902, <sup>3</sup>J<sub>PSn</sub> = 367 (<sup>119</sup>Sn), <sup>1</sup>J<sub>PH</sub> = 181, <sup>2</sup>J<sub>PP</sub> = 34, <sup>2</sup>J<sub>SnH</sub> = 27.7, <sup>3</sup>J<sub>PH</sub> = 1.5, <sup>4</sup>J<sub>SnH</sub> = 43.0; <sup>d</sup> **6**, <sup>1</sup>J<sub>PSn</sub> = 1349 (<sup>119</sup>Sn), 1298, <sup>3</sup>J<sub>PSn</sub> = 187 (<sup>119</sup>Sn), <sup>1</sup>J<sub>PH</sub> = 186, <sup>2</sup>J<sub>PP</sub> = 43, <sup>3</sup>J<sub>SnH</sub> = 88.6 (<sup>119</sup>Sn), 84.7 (<sup>117</sup>Sn), <sup>3</sup>J<sub>PH</sub> = 4.5; **7**, <sup>1</sup>J<sub>PSn</sub> = 1281 (<sup>119</sup>Sn), 1238, <sup>3</sup>J<sub>PSn</sub> = 82 (<sup>119</sup>Sn), <sup>1</sup>J<sub>PH</sub> = 180, <sup>3</sup>J<sub>HH</sub> = 6.7, <sup>3</sup>J<sub>SnH</sub> = 89.9 (<sup>119</sup>Sn), 86.1 (<sup>117</sup>Sn), <sup>3</sup>J<sub>PH</sub> = 4.0; **8**, <sup>1</sup>J<sub>PSn</sub> = 601 (<sup>119</sup>Sn), 585, <sup>3</sup>J<sub>SnH</sub> = 83.7 (<sup>119</sup>Sn), 80.3 (<sup>117</sup>Sn); **9**, <sup>1</sup>J<sub>PSn</sub> = 584 (<sup>119</sup>Sn), 550, <sup>3</sup>J<sub>SnH</sub> = 83.6 (<sup>119</sup>Sn), 80.4 (<sup>117</sup>Sn), <sup>3</sup>J<sub>HH</sub> = 6.7; **11**, <sup>1</sup>J<sub>PSn</sub> = 968 (<sup>119</sup>Sn), 894, <sup>3</sup>J<sub>PSn</sub> = 262 (<sup>119</sup>Sn), <sup>1</sup>J<sub>PH</sub> = 172, <sup>2</sup>J<sub>PP</sub> = 26. <sup>b</sup> Hexane solution. <sup>c</sup> The separate P-<sup>119</sup>Sn and P-<sup>117</sup>Sn couplings are not well-resolved in the <sup>31</sup>P NMR spectrum. <sup>d</sup> The separate H-<sup>119</sup>Sn and H-<sup>117</sup>Sn couplings are not well-resolved in the <sup>1</sup>H NMR spectrum.

**Scheme 1<sup>4</sup>**

g, 2.2 mmol) in hexane (30 mL) was cooled to -78 °C and <sup>t</sup>BuLi/pentane solution (1.3 mL, 2.2 mmol, 1.7 M solution) was added slowly with stirring through an air-tight syringe. The resulting cloudy orange solution was stirred at -78 °C (2 h) and at +23 °C (16 h) and then filtered. The filtrate was evaporated to dryness and the residue recrystallized from pentane at -10 °C, leaving orange crystals of **8**: yield, 0.70 g (54%); mp 146-148 °C (dec). Mass spectrum (30 eV) [*m/e* (%)]: 483-485 (M - <sup>t</sup>Bu<sup>+</sup>, 2%), 419-424 (55%), 362 (M - <sup>t</sup>Bu<sub>2</sub>Sn<sup>+</sup>, 100%). Infrared spectrum (KBr, cm<sup>-1</sup>): 2959 (s), 2930 (s), 2843 (s), 2712 (w), 1464 (m), 1379 (m), 1362 (m), 1310 (m), 1279 (s), 1241 (w), 1155 (s), 1125 (m), 1040 (w), 988 (m), 804 (w), 678 (w), 575 (w). Anal. Calcd for C<sub>26</sub>H<sub>54</sub>B<sub>2</sub>N<sub>2</sub>P<sub>2</sub>Sn (596.96): C, 52.31; H, 9.12; N, 4.69. Found: C, 52.47; H, 9.58; N, 4.71.

Compound **9** was prepared in an identical fashion: yield, 0.7 g (52%); mp 136-138 °C (dec). Mass spectrum (30 eV) [*m/e* (%)]: 513-522 (M<sup>+</sup>, 12%). Infrared spectrum (KBr, cm<sup>-1</sup>): 2965 (s), 2924 (s), 2839 (s), 2710 (w), 1462 (s), 1433 (s), 1364 (s), 1294 (s), 1184 (m), 1144 (s), 1030 (m), 804 (w), 770 (w), 669 (w), 571 (m). Anal. Calcd for C<sub>20</sub>H<sub>46</sub>B<sub>2</sub>N<sub>2</sub>P<sub>2</sub>Sn (516.84): C, 46.48; H, 8.97; N, 5.42. Found: C, 46.28; H, 9.26; N, 5.26.

**Dimethylbis[2,4-bis(2,2,6,6-tetramethylpiperidino)-1,3-diphospho-2,4-diboretanyl]stannane (11).** A sample of **4** (0.75 g, 1.6 mmol) was combined with Me<sub>2</sub>SnCl<sub>2</sub> (0.17 g, 0.77 mmol) in hexane (30 mL) at -78 °C and stirred at -78 °C (2 h) and at +23 °C (16 h) and then filtered. The filtrate was vacuum evaporated to dryness and the residue recrystallized from hexane (10 mL) at -10 °C, leaving pale orange

crystals of **11**: yield, 0.45 g (63%); mp 179–181 °C. Mass spectrum (HR-FAB): calcd for  $C_{38}H_{80}N_4^{11}B_2^{10}P_4^{120}Sn$ , 878.480 038; found 878.480 95 (dev, -0.1 ppm). Infrared spectrum (hexane,  $cm^{-1}$ ): 2228 (s), 1448 (w), 1398 (m), 1325 (s), 1302 (s), 1242 (m), 1169 (s), 1130 (m), 1088 (w), 1044 (w), 993 (s), 866 (w), 817 (w), 747 (m), 573 (w), 503 (w). Anal. Calcd for  $C_{38}H_{80}N_4B_4P_4Sn$  (878.87): C, 51.93; H, 9.18; N, 6.38. Found: C, 53.53; H, 9.52; N, 6.14.

**2:1 Reactions of 3 and 4 with  ${}^tBu_2SnCl_2$ .** A 2 equiv amount of **3** or **4** was combined with 1 equiv of  ${}^tBu_2SnCl_2$  (1.0 mmol) in hexane (50 mL) at -78 °C and stirred at -78 °C (2 h) and +23 °C (16 h). The resulting mixtures were filtered to remove LiCl and the filtrates evaporated to dryness, leaving orange solids. Analysis by  ${}^{31}P$  and  ${}^1H$  NMR revealed that the solids were 1:1 mixtures of **9** and **1** or **8** and **2**.

**1:1 Reaction of 5 with  ${}^tBuLi$ .** Combination of **5** (0.35 g, 0.64 mmol) with a  ${}^tBuLi$ /pentane solution (0.38 mL, 1.7 M solution, 0.65 mmol) at -78 °C gave a cloudy orange solution which was stirred (2 h) and warmed to +23 °C and stirred (16 h). The mixture was filtered to remove LiCl and vacuum evaporated, leaving a pale yellow glassy solid. Mass spectrum (FAB): ion envelopes in the range  $m/e$  555–2246.

**Crystallographic Measurements and Structure Solutions.** Crystals of **8** and **9** were obtained as described above. Crystals of each were placed in glass capillaries under a dry nitrogen atmosphere and sealed. The crystals were centered on a Syntex P3/F automated diffractometer and determinations of crystal class, orientation matrix and unit cell dimensions were performed in a standard manner. Data were collected in the  $\omega$  scan mode with Mo  $K\alpha$  ( $\lambda = 0.71073$  Å) radiation, a scintillation counter, and pulse height analyzer. Inspection of small data sets led to the assignments of the space groups.<sup>9</sup> Empirical absorption corrections were applied on the basis of  $\psi$  scans.<sup>10</sup> No signs of crystal decay were noted.

All calculations were performed on a Siemens SHELXTL PLUS structure determination system.<sup>11</sup> Solutions for the data sets were by direct methods (**8**) and heavy atom techniques (**9**). Full matrix least-squares refinements were employed,<sup>12</sup> and neutral atom scattering factors and anomalous dispersion terms were used for all non-hydrogen atoms during the refinements. The data collection and refinements for **8** proceeded in a normal fashion. The heavy atom positions were refined anisotropically, and H atom positions were computed by using the riding model with isotropic  $U^s$  set at  $1.25U_{equiv}$  of the parent atom. Compound **9** displayed disorder in the  ${}^tBu$  group containing C(18), C(19), and C(20). Site occupancies were varied, leading to occupancies of 0.61 (primary) and 0.39 (secondary). All heavy atoms in the final refinement were allowed to vary anisotropically in position except C(18), C(19), and C(20), which were fixed in occupancy and position. The  $U_{iso}$ 's were allowed to vary for these three atoms.

Listings of selected data collection and crystal data are provided in Table 2, and pertinent bond distances and angles are summarized in Table 3. Additional crystallographic data, heavy atom coordinates, hydrogen atom coordinates, anisotropic thermal parameters, and full listings of bond lengths and angles are provided in Supporting Information.

(9) Space group notation is given in: *International Tables for X-ray Crystallography*; Reidel: Dordrecht, Holland, 1983; Vol. I, pp 73–346.

(10) The empirical absorption corrections use an ellipsoidal model fitted to azimuthal scan data that are then applied to the intensity data: *SHELXTL Manual*, Revision 4; Nicolet XRD Corp.: Madison, WI, 1983.

(11) Sheldrick, G. M. *Nicolet SHELXTL Operations Manual*; Nicolet XRD Corp.: Cupertino, CA, 1981. SHELXTL uses absorption, anomalous dispersion, and scattering data compiled in: *International Tables for X-ray Crystallography*; Kynoch: Birmingham, England, 1974; Vol. IV, pp 55–60, 99–101, 149–150. Anomalous dispersion terms were included for all atoms with atomic numbers greater than 2.

(12) A general description of the least-squares algebra is found in: *Crystallographic Computing*; Ahmed, F. R., Hall, S. R., Huber, C. P., Eds.; Munksgaard: Copenhagen, 1970; p 187. The least-squares refinement minimizes  $\sum w(|F_o| - |F_c|)^2$ , where  $w = 1/[\sigma(F_o)^2 + gF_o^2]$ .  $R = \sum(|F_o| - |F_c|)/\sum|F_o|$ ,  $R_w = [\sum w(|F_o| - |F_c|)^2/\sum wF_o^2]^{1/2}$ , and  $GOF = [\sum w(|F_o| - |F_c|)^2/(NO - NV)]^{1/2}$ , where NO = number of observations and NV = number of variables.

**Table 2.** Crystallographic Data for  $P_2(tmpB)_2Sn^tBu_2$  (**8**),  $P_2(Pr_2NB)_2Sn^tBu_2$  (**9**), and  $[HP(tmpB)_2P]_2SnMe_2$  (**11**)

	<b>8</b>	<b>9</b>
chem formula	$C_{26}H_{54}B_2N_2P_2Sn$	$C_{20}H_{46}B_2N_2P_2Sn$
fw	597.0	516.8
cryst syst	monoclinic	monoclinic
space group	$P2_1/c$	$P2_1/c$
$a$ , Å	11.369(1)	10.818(1)
$b$ , Å	12.342(1)	25.992(2)
$c$ , Å	22.573(2)	10.870(1)
$\alpha$ , deg	90	90
$\beta$ , deg	93.22(1)	111.34(1)
$\gamma$ , deg	90	90
$V$ , Å <sup>3</sup>	3162.2(4)	2847.1(4)
$Z$	4	4
$D_{calcd}$ , g $cm^{-3}$	1.254	1.206
$T$ , °C	20	20
$\mu$ , $cm^{-1}$	9.25	10.17
$\lambda(Mo K\alpha)$	0.710 73	0.710 73
$R_F^a$ (%)	3.64	3.69
$R_{wF}^b$ (%)	2.83	3.84
	$F > 2\sigma(F)$	$F > 3\sigma(F)$

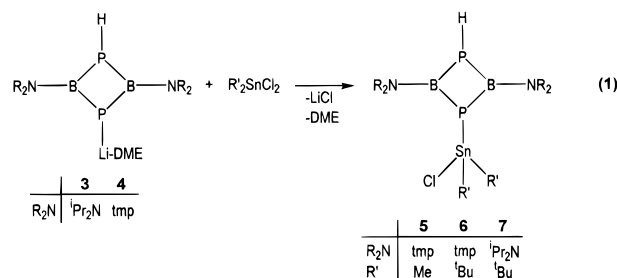
$$^a R_F = \sum(|F_o| - |F_c|)/\sum|F_o|. \quad ^b R_{wF} = [\sum w(|F_o| - |F_c|)^2/\sum wF_o^2]^{1/2}.$$

**Table 3.** Selected Bond Lengths (Å) and Angles (deg) for **8** and **9**

	<b>8</b>		<b>9</b>	
B–P	P(1)–B(1)	1.985(6)	P(1)–B(1)	1.981(4)
	P(1)–B(2)	1.976(5)	P(1)–B(2)	1.987(5)
	P(2)–B(1)	1.991(5)	P(2)–B(1)	1.960(4)
Sn–P	P(2)–B(2)	1.993(6)	P(2)–B(2)	1.960(6)
	Sn–P(1)	2.527(1)	Sn–P(1)	2.520(1)
	Sn–P(2)	2.537(1)	Sn–P(2)	2.527(1)
B–N	B(1)–N(1)	1.403(6)	B(1)–N(1)	1.390(5)
	B(2)–N(2)	1.405(6)	B(2)–N(2)	1.394(8)
Sn–C	Sn–C(19)	2.202(5)	Sn–C(13)	2.205(6)
	Sn–C(23)	2.209(5)	Sn–C(17)	2.210(4)
B–P–B	B(1)–P(1)–B(2)	72.8(2)	B(1)–P(1)–B(2)	65.2(2)
	P(1)–P(2)–B(2)	72.3(2)	P(1)–P(2)–B(2)	66.1(2)
P–B–P	P(1)–B(1)–P(2)	98.7(2)	P(1)–B(1)–P(2)	103.2(2)
	P(1)–B(2)–P(2)	98.9(2)	P(1)–B(2)–P(2)	102.9(3)
P–Sn–P	P(1)–Sn–P(2)	73.1(1)	P(1)–Sn–P(2)	75.4(1)
	B(2)–P(1)–Sn	76.5(2)	B(2)–P(1)–Sn	76.5(2)
	B(1)–P(2)–Sn	76.5(2)	B(1)–P(2)–Sn	75.9(1)
	B(2)–P(2)–Sn	76.0(1)	B(2)–P(2)–Sn	76.8(2)

## Results and Discussion

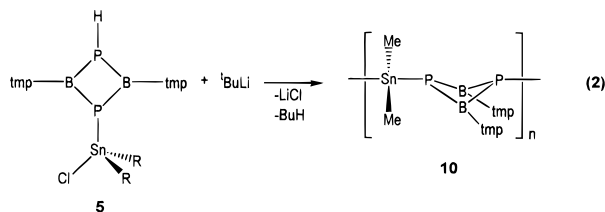
In the current study, the reactions of  ${}^iPr_2NBP(H)({}^iPr_2NB)P\text{-}Li\cdot DME$  (**3**) and  $(tmp)BP(H)(tmpB)PLi\cdot DME$  (**4**) with  $Me_2SnCl_2$  and  ${}^tBu_2SnCl_2$  in a 1:1 ratio have been examined as summarized in eq 1. The P-stannylated diphosphadiboretanes



**5–7** were isolated in good yield as crystalline air and moisture sensitive solids. The 1:1 reaction of **3** and  $Me_2SnCl_2$  was also examined, and an impure yellow oil was obtained. Attempts to purify the anticipated product,  ${}^iPr_2NBP(H)({}^iPr_2NB)PSn(Cl)Me_2$ , by vacuum distillation and crystallization were unsuccessful, and the compound was characterized only by  ${}^{31}P\{^1H\}$  NMR spectroscopy.

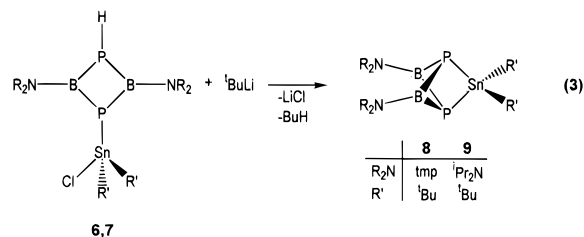
The mass spectrum of **6** shows a weak parent ion envelope in the mass range  $m/e$  631–636 with intensities that correspond to the expected isotope distribution. The mass spectra of **5** and **7** do not display a parent ion envelope, but **5** shows a fragment ion envelope at  $m/e$  509–514 corresponding to  $[M - Cl]^+$  and **7** shows an envelope at  $m/e$  493–500 consistent with a  $[M - 'Bu]^+$  fragment. The infrared spectra display a weak  $\nu_{PH}$  band in the region 2238–2278  $cm^{-1}$ , which is in the range of values observed for the boryl,<sup>1</sup> silyl,<sup>2</sup> and germyl<sup>3</sup> analogs of **5**–**7**. Similar to the B, Si, and Ge analogs, the <sup>31</sup>P NMR spectra (Table 1) of **5**–**7** show two resonances of equal intensity. The downfield resonance in each case is assigned to the diborylphosphane fragment ( $B_2PH$ ) since it splits into a widely spaced doublet ( $^1J_{PH} = 180$ – $186$  Hz) in the proton coupled spectra. The upfield resonance is assigned to the  $B_2PSn$  fragment on the basis of its P–Sn coupling satellites and lack of  $^1J_{PH}$  splitting. It is interesting that the  $^1J_{PSn}$  value for **5** ( $^1J_{PSn} = 902$  Hz) is significantly smaller than the values in **6** and **7** ( $^1J_{PSn} = 1298$  and  $1238$  Hz, respectively). In addition, the P–P' coupling is resolved with **5**,  $^2J_{PP'} = 34$  Hz, and **6**,  $^2J_{PP'} = 43$  Hz, but not in **7**. The  $^{119}Sn\{^1H\}$  NMR spectra for **5**–**7** show a single resonance centered at  $\delta$  75.1, 74.9, and 99.5, each split into a doublet of doublets by  $^1J_{PSn}$  coupling (920–1349 Hz) and  $^3J_{PSn}$  coupling (82–367 Hz). The chemical shifts for the four-coordinate Sn environments are intermediate in the range of shifts reported for  $Me_3SnPPh_2$ <sup>13</sup>  $\delta$  –2.3,  $Me_2Sn(PPh_2)_2$ <sup>14,15</sup>  $\delta$  –11.5, and  $(TMS_2CH)_2Sn(F)P(H)Ar$ <sup>16</sup>  $\delta$  +126.3. The  $^{11}B\{-^1H\}$  NMR spectra contain a single, relatively broad resonance centered at  $\delta$  49.9, 51.4, and 49.8, respectively, and these values are comparable with the B,<sup>1</sup> Si,<sup>2</sup> and Ge<sup>3</sup> analog species. The  $^1H$  and  $^{13}C\{^1H\}$  NMR spectra are consistent with the proposed structures of **5**–**7**. Of particular interest are the  $^1H$  NMR spectra that show a doublet centered in the range  $\delta$  3.9–4.7 with  $^1J_{PH} = 180$ – $190$  Hz, and as seen in a number of other compounds the  $^3J_{SnH}$  ( $\sim 90$  Hz) coupling constants are larger than the  $^2J_{SnH}$  ( $\sim 30$  Hz) coupling constants.<sup>17</sup>

The dehydrohalogenation of **5**–**7** with  $tBuLi$  was examined. In the case of **5**, with small substituent groups on the Sn atom, an oligomeric solid **10** was obtained, as described in eq 2. A



similar intermolecular elimination/condensation dehydrogenation oligomer was obtained with  $GeMe_2$ .<sup>3</sup> The oligomer **10** was studied by FAB-MS analysis and found to give ions out to at least  $m/e$  2246, which indicates that  $n > 4$ . The oligomer is soluble in benzene, and it shows broad resonances in the <sup>31</sup>P NMR spectrum between –100 and –150 ppm. Further characterization of the oligomer has not been attempted.

Compounds **6** and **7**, with larger  $tBu$  groups on the Sn atom, undergo intramolecular dehydrohalogenation with formation of the bicyclo[1.1.1] cage species **8** and **9**, as shown in eq 3.<sup>18</sup>



This process was also observed with Si<sup>2</sup> and Ge<sup>3</sup> analogs carrying larger R' groups than Me. Compounds **8** and **9**, however, are noticeably less thermally stable than the Si and Ge analogs as the tin derivatives decompose above 140 °C. Further, **8** shows no parent ion in the EI mass spectrum, and **9** gives only a weak parent ion. For the Si and Ge species, the parent ion was usually the most intense ion.

The NMR data for **8** and **9** are comparable with the spectral features for the B, Si, and Ge analogs, and they are consistent with the proposed cage structure. The  $^{11}B\{^1H\}$  NMR spectra contain a single resonance: **8**,  $\delta$  +49.7; **9**,  $\delta$  +49.1. The  $^{31}P\{-^1H\}$  NMR spectra show a single resonance at significantly lower field than the precursor molecules: **8**,  $\delta$  +50.1; **9**,  $\delta$  –12.7. This trend was also found with the B, Si, and Ge analogs. With the tin compounds, however, the resonance shows one bond Sn–P coupling: **8**,  $^1J_{SnP} = 585$  Hz; **9**,  $^1J_{SnP} = 550$  Hz. The  $^{119}Sn\{^1H\}$  NMR spectra for **8** and **9** display a triplet due to coupling with the two equivalent phosphorus atoms: **8**,  $\delta$  –277.0; **9**, –197.1. These shifts are significantly upfield of the precursors **6** and **7**, and the  $^1J_{SnP}$  coupling constants are about half the values found in **6** and **7**. The reduced coupling constants reflect a smaller degree of s orbital character in the P–Sn bonds in the cages, and the X-ray crystallographic data *vide infra* support this conclusion.

The molecular structures of **8** and **9** were determined by single crystal X-ray diffraction analysis. Views of the molecules are shown in Figures 1 and 2, and selected bond distances and angles are summarized in Table 3. Both molecules have a trigonal-bipyramidal cage structure with the phosphorus atoms in the apical positions, as found with the  $P_2B_3$ ,<sup>1</sup>  $P_2B_2Si$ ,<sup>2</sup> and  $P_2B_2Ge$ <sup>3</sup> cage compounds, except that the P–Sn–P bond angle is much smaller due to the larger size of the Sn atom. The P–Sn–P angle in **9** is slightly larger, 75.4°, than in **8**, 73.1°, and this is accompanied by a less acute average P–B–P angle in **9**, 103.1°, than in **8**, 98.8°. The average internal angles at the phosphorus atoms are very acute as in the cases of the other cage species: **8**, 75.2°; **9**, 72.9°. The average B–P–B angle is significantly more acute in **9** (65.6°) than in **8** (72.5°). The average B–P bond lengths (**8**, 1.986 Å; **9**, 1.972 Å) fall in the single bond range,<sup>19</sup> and they are comparable with the values

(18) Compound **8** was also obtained but in an impure state by reaction of equimolar amounts of  $((tmp)BPk)_2$  (0.56 g, 1.5 mmol) and  $tBu_2SnCl_2$  (0.48 g, 1.5 mmol) in benzene. The resulting red suspension was filtered and orange crystals of **8** (0.48 g, 53%) separated from the filtrate: mp 140–150 °C. An oily residue adhered tenaciously to these crystals. Several recrystallizations from hot benzene led to separation of colorless crystals which turned out to be  $[tBu_2Sn]_4$ .<sup>22</sup> Characterization data for **8** obtained in this fashion are essentially identical to those described in the Experimental Section. Small differences in NMR data likely result from solvent and concentration effects and from the fact that data were obtained on different instruments. Mass spectrum (70 eV) [ $m/e$  (%): 541 ( $M - tBu^+$  3%), 485 ( $M - 2tBu^+$  5%), 364 ( $M - Sn^+Bu_2^+$  100%), 349 ( $((tmp)BP)_2 - Me^+$  59%)].  $^{31}P\{^1H\}$  NMR ( $C_6D_6$ ):  $\delta$  50.4 (d,  $^1J_{119Sn-P} = 595$  Hz,  $^1J_{117Sn-P} = 570$  Hz).  $^{11}B\{^1H\}$  NMR ( $C_6D_6$ ):  $\delta$  48.9.  $^{119}Sn$  NMR ( $C_6D_6$ ):  $\delta$  –272.6 (t,  $^1J_{119Sn-P} = 595$  Hz).  $^{13}C\{^1H\}$  NMR ( $C_6D_6$ ):  $\delta$  37.9 ( $CM_3$ ), 33.7 ( $CM_3$ ), 58.3, 40.9, 34.8, 32.8, 15.9 (tmp). Similar reactions of  $((tmp)BPk)_2$  with  $Me_2SnCl_2$  and  $tPr_2SnCl_2$  in benzene gave yellow solutions from which insoluble yellow powders separated. The chloride free materials decomposed above 150 °C and were not characterized.

(13) McFarlane, W.; Rycroft, C. S. *J. Chem. Soc., Dalton Trans.* 1974, 1977.

(14) Kennedy, J. D.; McFarlane, W. Unpublished results.

(15) Harris, R. K.; Mann, B. E. *NMR and the Periodic Table*; Academic Press: New York, 1978.

(16) Couret, C.; Escudie, J.; Satge, J.; Rohariririna, A.; Andramizaka, J. D. *J. Am. Chem. Soc.* **1985**, *107*, 8280.

(17) Mason, J. *Multinuclear NMR*; Plenum Press: New York and London, 1987; Chapter 11.

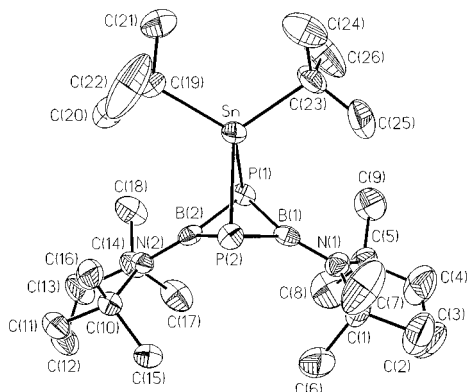


**Figure 1.** Atomic structure and atom labeling scheme for  $P_2(\text{tmpB})_2\text{-Sn}'\text{Bu}_2$  (**8**) with H atoms omitted (50% probability ellipsoids).

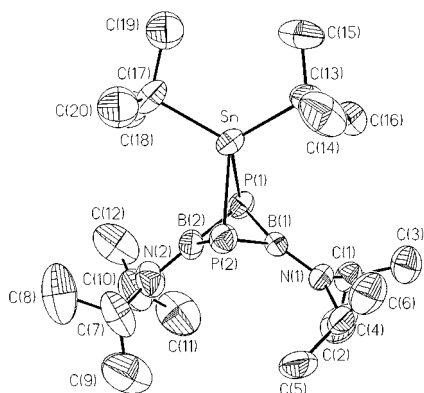
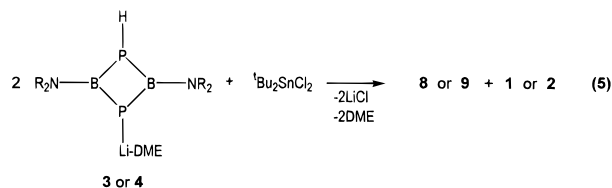
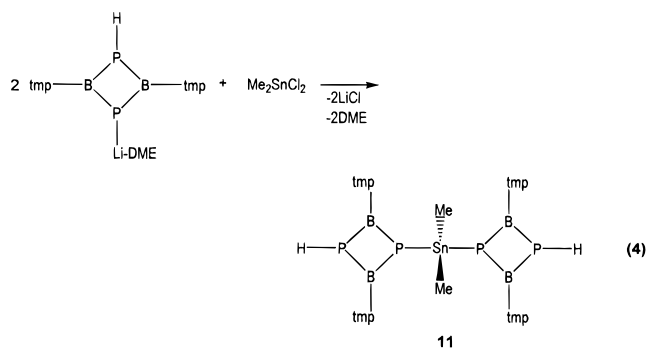


**Figure 2.** Atomic structure and atom labeling scheme for  $P_2(i\text{Pr}_2\text{-NB})_2\text{Sn}'\text{Bu}_2$  (**9**) with H atoms omitted (50% probability ellipsoids).

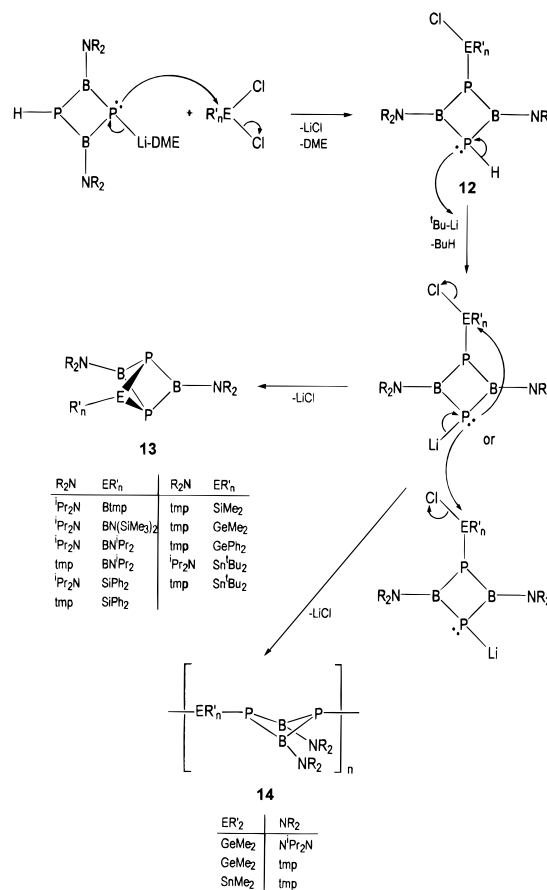
found in the  $P_2B_2Si$  and  $P_2B_2Ge$  cages. The average P–Sn distances (**8**, 2.532 Å; **9**, 2.524 Å) are similar to the average distance in  $[\text{Me}_2\text{Sn}]_6\text{P}_4$ , 2.51 Å.<sup>20</sup>

Given the different dehydrohalogenation reaction pathways displayed by **5** compared to **6** and **7**, it was of interest to explore the 2:1 stoichiometry reactions of **3** and **4** toward  $\text{Me}_2\text{SnCl}_2$  and  ${}^t\text{Bu}_2\text{SnCl}_2$ . The results are summarized in eqs 4 and 5.



With the combination of **4** and  $\text{Me}_2\text{SnCl}_2$  the bis(1,3-diphospha-2,4-diboretanyl)dimethyltin compound **11** was obtained. This

## Scheme 2



is consistent with the smaller steric demands of the methyl groups on the tin atom. Combination of **3** or **4** with  ${}^t\text{Bu}_2\text{SnCl}_2$ , however, produced the cage compound **8** or **9** and the 1,3-diphospha-2,4-diboretane **1** or **2**. This suggests that the substitution products **6** and **7** are initially formed and then the second equivalent of **3** or **4** acts as a dehydrohalogenation promoter. This chemistry has also been observed in the related chemistry on  $\text{R}'_2\text{GeCl}_2$  reagents where R' is bulky.<sup>3</sup>

Compound **11** was fully characterized by analytical and spectroscopic techniques. The compound displays a cluster of ions corresponding to the parent ion, and it shows a band at  $2228\text{ cm}^{-1}$  in the IR spectrum that is assigned to  $\nu_{\text{PH}}$ . The  $^{119}\text{Sn}\{-^1\text{H}\}$  NMR spectrum displays a triplet,  $\delta$  26.2,  $^1J_{\text{SnP}} = 968\text{ Hz}$ , due to coupling of two equivalent phosphorus atoms bonded to the central Sn atom. Each of these peaks is further split into a triplet by coupling with the equivalent P–H phosphorus atoms,  $^3J_{\text{SnP}} = 262\text{ Hz}$ . The  $^{11}\text{B}\{-^1\text{H}\}$  NMR spectrum shows a single resonance centered at  $\delta$  +52.6. The  $^{31}\text{P}\{-^1\text{H}\}$  NMR spectrum displays two resonances,  $\delta$  –107.3 and –127.9. The one at lower field becomes a doublet,  $^1J_{\text{PH}} = 172\text{ Hz}$ , in the proton coupled spectrum, and the one at higher field shows satellites due to Sn–P coupling,  $^1J_{\text{SnP}} = 894\text{ Hz}$ .

Crystals of **11** were obtained; however, they were found to diffract weakly. As a result, full anisotropic refinement was not possible. An isotropic refinement confirmed the proposed connectivity, and the resulting structural parameters are included in the Supplementary Information.

## Conclusion

The  $P_2B_2E$  cage assembly chemistry revealed in our studies to date is summarized in Scheme 2. The dehydrohalogenation of examples of **12** is promoted by strong bases, e.g.,  ${}^t\text{BuLi}$ , and it can proceed by intramolecular or intermolecular processes to

(19) Paine, R. T.; Nöth, H. *Chem. Rev.* **1995**, *95*, 343.

(20) Dräger, M.; Mathiasch, B. *Angew. Chem., Int. Ed. Engl.* **1981**, *20*, 1029.

products. It is now apparent that when the E element is relatively small (e.g., B and Si), only intramolecular dehydrohalogenation of **12** occurs, giving the bicyclic cage compounds **13** irrespective of the steric volume of the  $R_2N$  or  $R'$  substituent groups. With larger E elements (e.g., Ge and Sn), cage species are formed when  $R'$  is large. In only three cases, when E is large (Ge and Sn) and  $R' = Me$ , have intermolecular dehydrohalogenations been found to dominate, forming oligomeric products. In one of these,  $R_2N = tmp$  and  $E = GeMe_2$  both intramolecular and intermolecular processes took place. Obviously, the influences of other substituent group combinations need to be examined to fully understand all of the factors controlling the selection of one reaction pathway over the other, and such chemistry will continue in our group. In addition, other approaches are available for cage construction, and one process involving the carbenoid fragment,  $R_2Sn$ , addition to the bicycle  $(R_2NBP)_2$ , will be described separately.<sup>21</sup>

**Acknowledgment** is made to the National Science Foundation (Grant CHE-9508668) and to the donors of the Petroleum Research Fund, administered by the American Chemical Society (R.T.P.). A NATO grant initiated the initial collaboration between the research groups in Albuquerque and Munich.

**Supporting Information Available:** Tables containing details of the X-ray data collection and refinement, heavy atom coordinates, hydrogen atom coordinates, thermal parameters, and complete listings of bond lengths and angles (43 pages). Ordering information is given on any current masthead page.

IC9612818

- 
- (21) Kaufmann, B.; Nöth, H.; Paine, R. T. Submitted for publication.  
(22) Puff, J.; Boch, C.; Schuh, W.; Zimmer, R. *J. Organometal. Chem.* **1986**, 312, 312.